AIP Journal of Applied Physics

Influence of microstructure on the enhancement of soft magnetic character and the induced anisotropy of field annealed HITPERM-type alloys

J. S. Blázquez, J. Marcin, M. Varga, V. Franco, A. Conde, and I. Skorvanek

Citation: Journal of Applied Physics **117**, 17A301 (2015); doi: 10.1063/1.4906173
View online: http://dx.doi.org/10.1063/1.4906173
View Table of Contents: http://scitation.aip.org/content/aip/journal/jap/117/17?ver=pdfcov
Published by the AIP Publishing

Influence of microstructure on the enhancement of soft magnetic character and the induced anisotropy of field annealed HITPERM-type alloys

J. S. Blázquez,[1] J. Marcin,[2] M. Varga,[2] V. Franco,[1,a)] A. Conde,[1] and I. Skorvanek[2]
[1]*Departamento de Física de la Materia Condensada, ICM-SE CSIC, Universidad de Sevilla, P. O. Box 1065, 41080 Sevilla, Spain*
[2]*Institute of Experimental Physics, Slovak Academy of Sciences, SK-040 01 Kosice, Slovakia*

(Presented 5 November 2014; received 4 September 2014; accepted 15 September 2014; published online 14 January 2015)

Hitperm-type rapidly quenched ribbons were submitted to field annealing, both longitudinal field (LF) and transversal field (TF) to the axis of the ribbon. LF annealing yields a reduction of the magnetic anisotropy and results can be explained in the frame of random anisotropy model. A coercivity of 3 A/m is obtained for $Fe_{39}Co_{39}Nb_6B_{15}Cu_1$ alloy. The addition of Cu to these Nb-containing Hitperm-type alloys is a key factor to refine the microstructure in order to reach this very low coercivity value. TF annealing produces samples with sheared hysteresis loops suitable for sensor and high frequency applications. © *2015 AIP Publishing LLC*.
[http://dx.doi.org/10.1063/1.4906173]

Soft magnetic nanocrystalline alloys are formed by ferromagnetic α-Fe type nanocrystals embedded in a residual amorphous matrix. As temperature increases above the Curie temperature of the amorphous phase (T_C^{Am}), the coupling between nanocrystals becomes deteriorated and the ultrasoft magnetic character of the system is lost. In 1998, Hitperm alloys (Fe-Co-*ETM*-B-Cu being *ETM* = Zr, Nb, Mo, Hf, etc.) were proposed as soft magnets for high temperature applications.[1] The key parameter of Hitperm alloys is a high T_C^{am}, which generally exceeds the onset of nanocrystallization temperature. Therefore, in order to achieve the nanocrystalline microstructure, Hitperm alloys have to be annealed below T_C^{am} implying a stabilization of the magnetic domain walls due to the pair ordering mechanism.[2,3] In general, this procedure leads to a magnetic hardening of the system.[4,5] However, it has been shown that field annealing is very effective to avoid this hardening in Hitperm alloys.[6–11] In fact, as the sample is magnetically saturated during the annealing process, stabilization of domain walls is avoided and coercivities below 10 A/m are obtained for longitudinal field (LF) annealed Hitperm alloys.

Amorphous ribbons (15 μm thick) of $Fe_{78-x}Co_xNb_6B_{16-y}Cu_y$ (x = 39, 60; y = 0, 1) were produced by melt-spinning. Pieces 60 mm long, 5 mm wide, and ~20 μm thick were annealed during 1 h at the peak temperature of the nanocrystallization process detected by differential scanning calorimetry (DSC) under three different conditions: (a) zero magnetic field (ZF), (b) applying 20 kA/m LF, and (c) applying 640 kA/m transversal field (TF) in the plane of the ribbon. Hysteresis loops were acquired using a Forster type B-H loop tracer based on flux-gate magnetometer.

In the Nb-containing Hitperm alloys with 39 at. % Co content, addition of 1 at. % Cu leads to a refinement of the microstructure and the average crystal size reduces from $D = 7.5$ nm to 5 nm after Cu addition, whereas crystalline fraction after the nanocrystallization remains unaffected ($X_C \sim 55\%$). However, for alloys with 60 at. % Co, crystalline fraction decreases ($X_C \sim 45\%$) due to exhaustion of Fe in the remaining amorphous matrix and $D = 5$ nm.[12]

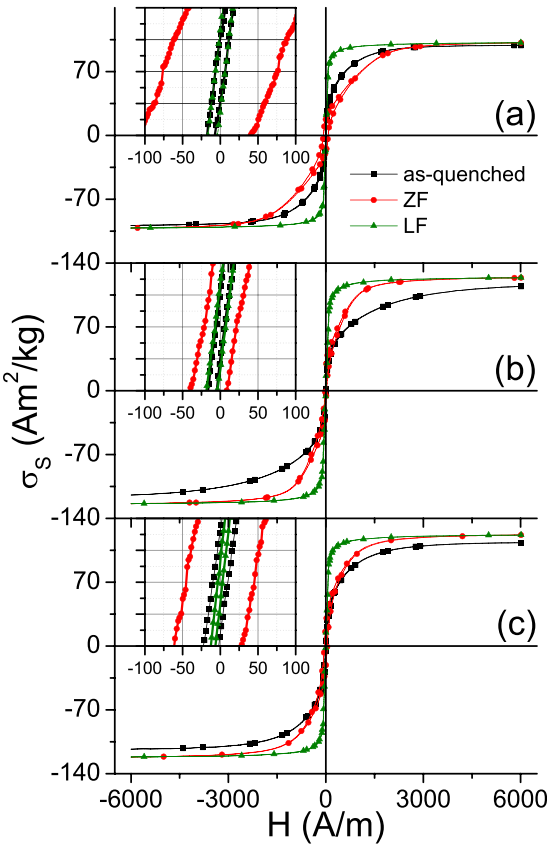

FIG. 1. Hysteresis loops of AQ amorphous and annealed nanocrystalline samples of $Fe_{78-x}Co_xNb_6B_{16-y}Cu_y$ alloys ((a) x = 39 and y = 1; (b) x = 39 and y = 0; (c) x = 18 and y = 1). Symbols are plotted each 25 data points to identify the curves. A magnified view is shown in the insets to appreciate the coercivity. Symbols in the inset correspond to individual $\sigma(H)$ data.

a)Author to whom correspondence should be addressed. Electronic mail: vfranco@us.es.

TABLE I. Parameters of nanocrystalline samples obtained after annealing at T_a.

Composition	T_a (K)	D (nm)	X_C (%)	Crystal phase composition	K_1 (kJ/m^3)	ρ (g/cm^3)
$Fe_{39}Co_{39}Nb_6B_{15}Cu_1$	739	5	55	$Fe_{0.61}Co_{0.39}$	~10	~8.1
$Fe_{39}Co_{39}Nb_6B_{16}$	766	7.5	55	$Fe_{0.61}Co_{0.39}$	~10	~8.1
$Fe_{18}Co_{60}Nb_6B_{15}Cu_1$	736	5	45	$Fe_{0.4}Co_{0.6}$	~−20	~8.3

Figure 1 shows the hysteresis loops of nanocrystalline samples of the three studied compositions for ZF and LF annealing along with the corresponding hysteresis loops of the as-quenched (AQ) amorphous alloy. It can be observed that LF samples exhibit a square hysteresis loop and show a clear softening of the magnetic character with respect to ZF annealed samples. A clear increase of saturation magnetization (M_S) is observed after nanocrystallization due to the formation of the α-FeCo phase. However, ZF annealed samples show a clear deterioration of the coercivity (H_C) with respect to AQ alloys due to the mechanism of pair ordering. Low coercivities of AQ samples are preserved or even improved after LF annealing (e.g., for x = 39, y = 1 alloy, $H_C = 3.1$ A/m compared to 9.8 A/m and 45 A/m for AQ and ZF samples).

The microstructural dependence of the observed magnetic data can be analyzed in the framework of the random anisotropy model considering its extension to two-phase systems.[13,14] In this context, the magnetocrystalline anisotropy averages out due to the small size of the crystallites (smaller than the exchange length) and it can be written as a function of the magnetocrystalline anisotropy, K_1, the exchange stiffness, A, and the microstructural parameters D and X_C[13]

$$\langle K \rangle = \left(\frac{3}{4}\right)^3 \frac{K_1^4 D^6}{A^3} {X_C}^2. \quad (1)$$

This expression predicts a decrease of the average magnetic anisotropy, $\langle K \rangle$, and thus of H_C, as D decreases, which is in agreement with the observed difference between H_C values for 39 at. % Co alloys with and without Cu. These two systems have the same volume fraction and composition of the crystalline phase but a larger D is observed for the Cu-free alloy. The change in the effective magnetic anisotropy, $K_{eff} \sim \mu_0 M_S H_C$, can be compared to the expected change of this averaged anisotropy $\langle K \rangle$. A simple calculation imposing $K_1 \sim 10$ kJ/m^3 (Ref. 15) for a $Fe_{0.61}Co_{0.39}$ composition and the microstructural parameters collected in Table I leads to a value of $A \sim 0.5 \times 10^{-11}$ J/m, which is in good agreement with the expected value.

The two studied Cu-containing alloys show $D = 5$ nm. In the case of the alloy with 60 at. % Co, a decrease in X_C with respect to the alloy with 39 at. % Co alloys should imply a decrease in $\langle K \rangle$ for a constant value of $D = 5$ nm, in disagreement with the observed trend. The explanation for this apparent contradiction is the different composition of the crystalline phases, which yields different values of K_1. In fact, expression (1) shows a stronger dependence on K_1 than on X_C. The value of K_1 depends on the composition of the α-FeCo phase, being ~50 kJ/m^3 for pure α-Fe and decreasing as Co content increases down to ~−40 kJ/m^3 for 70 at. % Co.[15] Therefore, assuming that the compositions of nanocrystals are $Fe_{0.61}Co_{0.39}$ and $Fe_{0.4}Co_{0.6}$ for the alloys with 39 and 60 at. % Co, respectively,[16] K_1 can be estimated as ~+10 kJ/m^3 and −20 kJ/m^3 for x = 39 and 60 alloys, respectively,[15] which explains the observed difference.

Figure 2 shows the hysteresis loops of TF annealed samples, which show sheared loops, almost linear up to the anisotropy field, H_k, where M_S is reached. This indicates that rotation of magnetic moments is the dominant mechanism for magnetization in these samples. Such type of hysteresis loops is especially interesting for sensor applications,

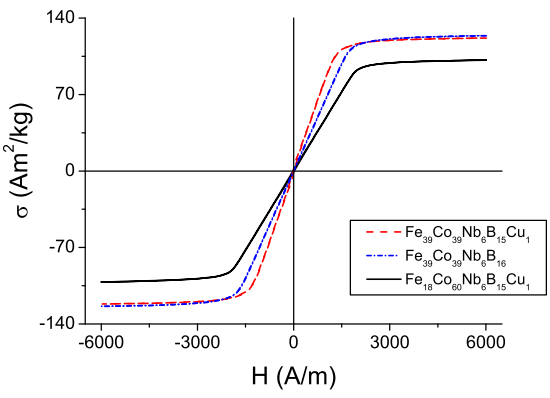

FIG. 2. Hysteresis loops of transversal field annealed samples of the three studied compositions.

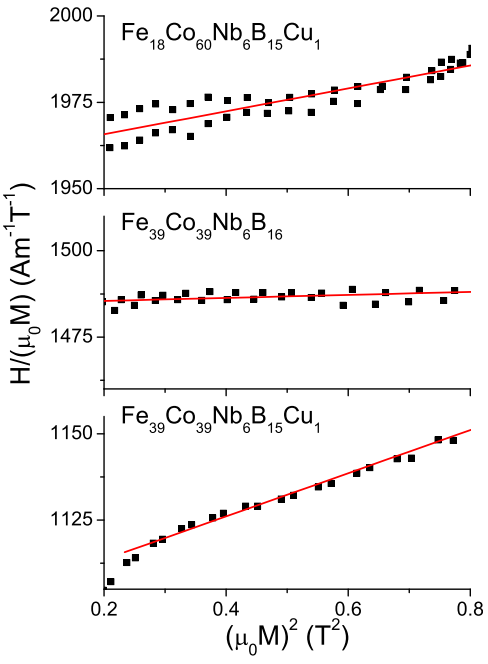

FIG. 3. Sucksmith-Thompson plot of the three studied compositions submitted to transversal field annealing. Lines correspond to linear fittings.

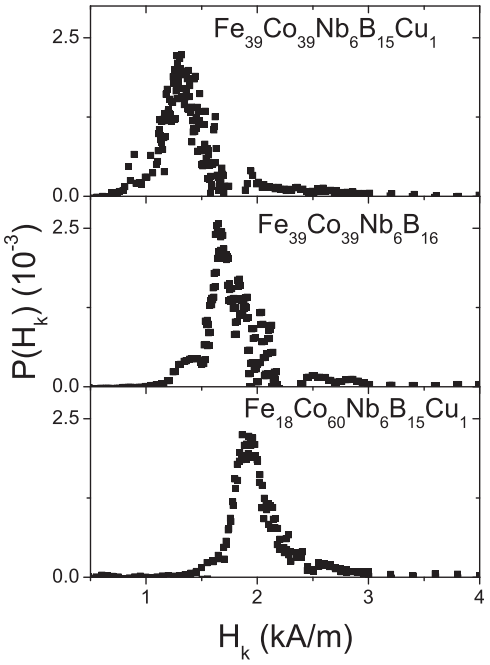

FIG. 4. Probability distribution of anisotropy fields from the second derivative of the magnetization curve from saturation to remanence (data shown correspond to a smoothing using ten neighboring points).

whereas the reduced susceptibility makes these samples interesting for high frequency transformer applications.[17]

In order to characterize the sensitiveness to TF annealing process, the induced magnetic anisotropy, K_u, has been characterized using several procedures. On the one hand, K_u can be directly estimated from the value of the anisotropy field, H_k, as: $K_u = \mu_0 M_S H_k/2$, where H_k has been estimated as the linear extrapolation to reach M_S. $K_u = 860$, 1170, and 1090 J/m^3 for x = 39, y = 1; x = 39, y = 0, and x = 18, y = 1 alloys, respectively.

On the other hand, the method of Sucksmith and Thompson[18] allows us to obtain the two first coefficients of the magnetic anisotropy K_{1u} and K_{2u} based on the relation

$$\frac{2K_{1u}}{(\mu_0 M_S)^2} + \frac{4K_{2u}}{(\mu_0 M_S)^4}\left(\mu_0 M(H)\right)^2 = \frac{H}{\mu_0 M(H)}, \qquad (2)$$

where $M(H)$ represents the magnetization at a given field H. Therefore, following expression (3), Figure 3 shows the plot of $H/(\mu_0 M)$ vs $(\mu_0 M)^2$ from which K_{1u} can be obtained from the value of the intercept with the y axis and K_{2u} from the slope of the curve. The obtained values are in agreement with the previous ones. $K_{1u} = 849.0(5)$, 1182.5(6), and 1108.7(8) J/m^3 for x = 39, y = 1; x = 39, y = 0, and x = 18, y = 1 alloys, respectively.

Finally, a study on the distribution of anisotropy fields, $P(H_k)$, can be done from the second derivative of the magnetization curve using the two branches from saturation to remanence, as it has been described for amorphous[19] and nanocrystalline systems[20]

$$P(H_k) = \frac{H}{M_S}\frac{d^2M(H)}{dH^2}. \qquad (3)$$

The corresponding plots are shown in Figure 4. There are no significant differences in the width of the distribution, although it is smaller in the alloy with the highest Co content. It can be observed that K_u follows the same trend than the residual K_{eff} observed in LF annealed samples and described above. The smallest value of K_u (or K_{u1}) is found for the alloy with 39 at. % Co and 1 at. % Cu, whereas the largest value of induced anisotropy is found for the Cu-free alloy.

In conclusion, the magnetic hardening observed in ZF nanocrystalline samples is prevented after field annealing in the saturation state and a minimum $H_C = 3$ A/m has been obtained for LF which equal the best H_C values reported up to date for $Fe_{38}Co_{38}Mo_8B_{15}Cu_1$ Hitperm alloys.[8] Microstructural and compositional differences between the studied alloys can explain the differences observed in their magnetic properties. On the other hand, whereas LF yields a minimization of $\langle K \rangle$ and square hysteresis loops, TF annealing produces samples with sheared hysteresis loops, which would be interesting for sensor and high frequency applications.

Work supported by NANOKOP Nr. ITMS 26110230061 NanoCEXmat Nr. ITMS 26220120019 projects, the Slovak Agency for the Research and Development (Project Nos. APVV-0266-10 and APVV-0492-11), MNT ERA NET II STREAM, the Spanish MINECO and EU FEDER (Project No. MAT 2013-45165-P), and the PAI of the Regional Government of Andalucía (Project No. P10-FQM-6462).

[1]M. A. Willard *et al.*, J. Appl. Phys. **84**, 6773 (1998).
[2]L. Néel, J. Phys. Radium **15**, 225 (1954).
[3]S. Taniguchi and M. Yamamoto, Sci. Rep. Res. Inst., Tohoku Univ., Ser. A **6**, 330 (1954).
[4]J. S. Blázquez *et al.*, J. Magn. Magn. Mater. **250**, 260 (2002).
[5]T. Kulik *et al.*, J. Alloys Compd. **434**, 623 (2007).
[6]I. Skorvanek *et al.*, J. Magn. Magn. Mater. **304**, 203 (2006).
[7]I. Skorvanek *et al.*, J. Magn. Magn. Mater. **310**, 2494 (2007).
[8]I. Skorvanek *et al.*, J. Alloys Compd. **504**, S135 (2010).
[9]I. Skorvanek *et al.*, Magnetohydrodynamics **48**, 371 (2012).
[10]F. Johnson *et al.*, IEEE Trans. Magn. **40**, 2697 (2004).
[11]K. Suzuki *et al.*, J. Non-Cryst. Solids **354**, 5089 (2008).
[12]J. S. Blázquez *et al.*, J. Phys.: Condens. Matter **14**, 11717 (2002).
[13]K. Suzuki and J. M. Cadogan, Phys. Rev. B **58**, 2730 (1998).
[14]A. Hernando *et al.*, Phys. Rev. B **51**, 3581 (1995).
[15]D. Bonnenberg *et al.*, in 1.2.1.2.7 Magnetocrystalline anisotropy edited by H. P. J. Wijn, *Landolt-Börnstein Database* Vol. 19a (Springer, Heidelberg, 1986), p. 210.
[16]Y. Zhang *et al.*, Mater. Sci. Eng. A **353**, 158 (2003).
[17]A. M. Leary *et al.*, JOM **64**, 772 (2012).
[18]K. H. J. Buschow and F. R. de Boer, *Physics of Magnetism and Magnetic Materials* (Kluwer Academic/Plenum Publishers, London, 2003), p. 99.
[19]J. M. Barandiarán *et al.*, IEEE Trans. Magn. **25**, 3330 (1989).
[20]V. Franco *et al.*, J. Magn. Magn. Mater. **185**, 353 (1998).